# Influence of Temperature Gradient on the Electromigration - Failures in 3D Packaging

**Ramdev Kanapady***
MSCWorks Inc,
ramdev@mscworks.net

**Darryl Moore, Arun Raghupathy and William Maltz**
Electronic Cooling Solutions Inc,
2915 Copper Road,
Santa Clara, CA 95051, USA
dmoore@eccoling.com

## ABSTRACT

In this paper, influence of temperature gradient in interconnects due to Joule heating in 3D packaging on electromigration failure is presented. Black's Mean Time to Failure (MTF) model relates exponentially to the temperature of interconnects which is assumed to be constant hence does not take into account temperature gradient. The developed electromigration model incorporates the driving force due to temperature gradient in addition to the effects of current density, vacancy concentration gradients and stress gradients in the interconnects and due to coefficient of thermal expansion mismatch with surrounding materials. Effectiveness of the developed finite element model is illustrated complex C4 solder bumps of flip-chip packages using COMSOL Mutliphysics® software. It is shown that for same current density in the complex C4 solder bumps of flip-chip packages it is possible that failure times could be lower for lower solder average temperature with higher temperature gradient than for higher solder temperature with low temperature gradient.

**KEY WORDS:** Electromigration, Solder joints, Flip-Chip packages, Global interconnects.

## NOMENCLATURE

| | |
|---|---|
| A | constant |
| B | Bulk modulus, $N/m^2$ |
| C | concentration |
| CTE | coefficient of thermal expansion, ppm/ $^oC$ |
| D | diffusivity, $m^2/s$ |
| Q | activation energy, eV |
| E | electric field, V/m |
| G | generation or annihilation source |
| K | thermal conductivity, W/mK |
| MTF | Mean Time for Failure, hr |
| Q* | heat of transport, eV |
| T | temperature, K |
| V | voltage, V |
| $Z^*$ | effective charge number |
| a | source length, m |
| e | elementary charge, C |
| f | vacancy relaxation factor |
| j | current density, $A/m^2$ |
| k | Boltzman constant, eV/K |
| l | length, m |
| x,y,z | co-ordinates |
| t | time, s |

**Greek symbols**

| | |
|---|---|
| $\rho$ | mass density ($kg/m^3$) |
| $\alpha$ | constant |
| $\beta$ | effective temperature, K |
| $\varepsilon$ | ratio of line cross section area to diffusion path |
| $\Omega$ | atomic volume, $m^3$/atom |
| $\nabla$ | gradient |
| $\Delta$ | divergence |
| $\sigma$ | hydrostatic stress, $N/m^2$ |

**Subscripts**

| | |
|---|---|
| a | activation energy |
| j | junction |
| h | hour |
| v | vacancy |

**Superscripts**

| | |
|---|---|
| n | constant |

## INTRODUCTION

The IC interconnects failure are caused by crack or void initiation and growth. Of the various failure mechanisms, electromigration (EM) [1] is one of main reasons. Electromigration is a critical problem, especially as the IC feature such as width and pitch of thin-film interconnects have been reduced to submicron-levels. In 3D packaging technology, EM can be due to drastic changes in geometries between metal wires, through-silicon-vias, and landing pads. Electromigration is also affected by recent changes in technology such as replacing aluminum with copper, replacing silica with low-k dielectrics, removing shunts, and adding capacitors. According to the International Technology Roadmap for Semiconductors (ITRS) update [2, 3], this continuous scaling down of on-chip interconnects, where high current densities and high temperature gradients are unavoidable, EM will be a critical reliability issue in the future and a model for reliable prediction of EM is a major necessity.

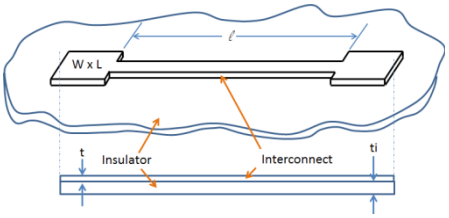


Fig. 1 Electromigration interconnect for accelerated testing.

Traditional EM failure prediction tools as iTEM [4], computes the overall reliability of a given interconnect layout based on individual straight line segments which are extracted from interconnect layouts. Straight-line resistor test specimens representing the interconnect of length $l$, width $w$ and thickness $t$ embedded in an insulator, such as the one shown in Fig. 1, are subjected to accelerated stress tests to characterize EM failure, where a number of such tests are carried out with high current density at a high temperature until they fail due to an open circuit. Current densities are increased in such tests to reduce the testing time for Joule heating that will increase the temperature and generate temperature gradients. These require special considerations if accurate characterization are to be made because EM failure are related exponentially to temperature Black's MTF model [1]. Modified form can be stated in Blair et al. [5]

$$MTF = \frac{A}{j^n} exp\left(\frac{Q}{kT}\right) \tag{1}$$

where MTF is Mean Time to Failure. If n is equal to 2, then Eq. 1 is the original Black's MTF model. If n is close or equal to 1 indicates that the significant portion of failure mechanism is dominated by void growth [6], while value of n6equal to 2 indicates failure mechanism life time is dominated by void nucleation [7]. The constant $A$ depends on interconnect geometry, material properties and can be temperature dependent.

In Eq. 1, the temperature gradient is not a parameter but it is well known the temperature gradient is a key driving force for EM (Eqs. 4-13 in the following section). Zhijian et al. [8] analyzed EM interconnects with both temporal and spatial temperature gradients and proposed which temperature to be used in the Eq. 1 for reliability calculations. For temporal temperature gradient situation, reliability equivalent temperature/current densities were proposed. For spatial temperature gradient situation, bounding temperatures were proposed to give upper and lower bounds for the lifetimes. This was based on the stress evolution Eq. 3 which accounts for temperature gradients in the interconnects and based on the following back flow of hydrostatic stress evolution equation during the vacancy transport given by Korhonen et al. [7].

$$\frac{\partial \bar{\sigma}}{\partial t} - \beta(T)\frac{\partial}{\partial x}\left(\frac{\partial \bar{\sigma}}{\partial x} - \bar{\alpha}(j)\right) \tag{2}$$

where $\beta(T) = D(B\Omega/kTl^2\varepsilon)$ is function of temperature and $\alpha(j) = Z^*l\rho j/\Omega$ is function of current density. Equation 2 is modified to include the temperature gradient as

$$\frac{\partial \bar{\sigma}}{\partial t} - \beta(T)\frac{\partial}{\partial x}\left(\frac{\partial \bar{\sigma}}{\partial x} - \bar{\alpha}(j)\right) - \frac{\partial \beta(T)}{\partial x}\left(\frac{\partial \bar{\sigma}}{\partial x} - \bar{\alpha}(j)\right) \tag{3}$$

Proposed temperature bound approach is limited to two-terminal interconnects such as in global signal interconnects and power/ground distribution networks [8] and it is also not clear how this model can applied to interconnect application where stress build due to CTE mismatch and spatial thermal gradients in the packages

Thematique [9] observed that for C4 solder bumps of flip-chip packages failure times could be lower for lower junction temperature with higher temperature gradient than for higher junction temperature with low temperature gradient. Case study considered three operating conditions for C4 solder bump with same current density but have different failure times. The results are summarized in Table 1. The operating condition, where temperature gradient is higher (case 2) has early EM failure even when the junction temperature is lower compared to case 3.

Hence the interconnects such as global tier interconnects [10] and C4 solder bumps [11, 12] which are on side of substrates that are far away from the heat sinks which is part of thermal management can have significant temperature gradients that can cause EM failure. In this paper, EM model that incorporates the driving force due to temperature gradient in addition to the effects of current density and vacancy concentration gradients is illustrated. Effectiveness of the developed finite element model is illustrated for complex geometry solder C4 bumps of flip-chip packages. The main goal is to show that temperature gradient is a critical parameter for failure times in addition to the temperature of interconnects.

Table 1.EM results for solder bumps from reference [4] with ambient temperature $T_a$ = 25ºC, current $I$ = 240 mA and current density $J$ = 0.12 mA/m$^2$.

| Parameters | Case 1 | Case 2 | Case 3 |
|---|---|---|---|
| Current density | 0.12 | 0.12 | 0.12 |
| Temperature (ºC) | 30 | 156ºC | 164ºC |
| $\nabla T$ (ºC/µm) | 0.001 | 0.295 | 0.114 |
| Time (h) | 4968 | 180 | 2400 |
| EM failure | No | yes | No |

## ELECTROMIGRATION MODEL

Electromigration is the process of transport of material due to current in metal where vacancy of atoms needs to be tracked. The vacancy flux due to various driving forces such concentration gradient, current densities, thermal gradient and

mechanical stress gradient can be accounted by following coupled thermal-electrical-mechanical governing equations. The electric field and current density can obtained from

$$\nabla \cdot \left(\frac{\nabla V}{\rho}\right) = 0 \tag{4}$$

Temperature field and its gradient can be obtained by solving

$$-\nabla \cdot (K\nabla T) = \frac{|\nabla V|^2}{\rho} \tag{5}$$

where the electrical resistivity can be function of temperature can be defined linear relation

$$\rho = \rho_0(1 + a(T - T_0)) \tag{6}$$

The mechanical stress in the interconnects and effects of thermal gradients and CTE mismatch can be described by

$$-\nabla \cdot \sigma = \alpha E(T - T_{ref}) \tag{7}$$

Equations 4 – 7 are solved with appropriate terminal and ground boundary conditions (BC) for Eq. 15, temperature and heat flux BCs for Eq. 14, and mechanical constrains and traction BCs for Eq. 16. It is assumed here that electricity, temperature and stress are steady-state, however, Eqs. 4-7 can be easily extended to include time dependent effects. Vacancy flux with above effects can be written as

$$J_v = J_{vc} + J_{vE} + J_{vT} + J_{v\sigma} \tag{8}$$

where *Jv* is the vacancy flux due concentration gradient given by

$$J_{vc} = -D_v \nabla C_v \tag{9}$$

Where $D_v$ is given by Arrhenius equation

$$D_v = D_0 exp\left(-\frac{Q}{RT}\right) \tag{10}$$

vacancy flux due to electric field/current density is given by

$$J_{vE} = \frac{|Z^*|e}{kT} EC_v = \frac{|Z^*|e}{kT} \rho j C_v \tag{11}$$

vacancy flux due to temperature gradient is given by

$$J_{vT} = D_v \frac{Q^*}{kT^2} C_v \nabla T \tag{12}$$

vacancy flux due to hydrostatic stress gradient is given by

$$J_{c\sigma} = -D_v \frac{f\Omega}{kT} C_v \nabla \bar{\sigma} \tag{13}$$

where hydrostatic stress is defied by

$$\bar{\sigma} = \frac{\sigma_x + \sigma_y + \sigma_z}{3} \tag{14}$$

The continuity equation for the vacancy concentration is given by

$$\frac{\partial C_v}{\partial t} + \nabla . \boldsymbol{J}_v = \boldsymbol{G} \tag{15}$$

where **G** is the source term which represents a generation and annihilation of vacancy concentration and can be function of stress evolution as in Eq. 2. Note in the absence of source term **G** (Eq. 9) and if the divergence of vacancy flux, $\nabla \cdot \boldsymbol{J}_v$ is equal to zero then rate of change of vacancy concentration is zero i.e. $\partial C/\partial t = 0$ hence no EM failure in the interconnects. Blocking BC is given by

$$D\left[\frac{\partial C_v}{\partial x} - \alpha C(0,t)\right] = 0 \tag{16}$$

where $\alpha = Z^* e \rho j L/kT$. This blocking BC for example, represents the boundaries for Aluminum-based interconnects with tungsten-filled vias where tungsten does not electromigrate. Also for example, the BC can represent boundaries of refractory barrier metal between the levels of copper interconnects. Instead of blocking BC, continuous supply of concentration BC can be specified as

$$C(l,t) = C_0 \tag{17}$$

with an initial condition of concentration as,

$$C(x,0) = C_0 \tag{18}$$

First we will highlight few results from literature that shows the relation between the above EM governing Eqs. 8-19 and MTF model Eq. 1. Shatzkes et al. [13] showed that considering only vacancy flux, ***Jv***, due to concentration gradient, current densities (Eqs. 9 and 11), and assuming failure occurs when the vacancy concentration reaches a given threshold value which is sufficiently higher than the initial vacancy concentration level, MTF model with current density exponent *n* of 2 ($MTF = AT^2/j^n\ exp(Q/kT)$) for semi-infinite EM line with the BCs in Eq. 16 and Eq. 17 is derived for large current density $|Z^*|e\rho j\sqrt{D_v t}/2kT \gg 0$. This is similar to Eq. 1 except for the multiplying term $T^2$ associated with constant A. Unlike Shatzkes et. al [13] who used critical vacancy concentration level as EM failure criteria, Korhonen

et al. [7], and Clement et al. [14] defined EM failure occur when the stress magnitude reaches given threshold value and showed that MTF has the form $MTF = A(T)/j^2 \exp(Q/kT)$ same as Blacks MTF model current density exponent of 2 and with $A(T)=AT^2$ for Korhonen et al. [7] formulation and $A(T)=AT^3$ for Clement et al. [14] formulation. While Korhonen et al. [7] used stress evolution Eq. 2, Clement et al. [14] used a simplified stress evolution equation in conjunction with Eq. 15 without considering vacancy flux due to temperature gradient Eq. 12 and stress gradient Eq. 13.

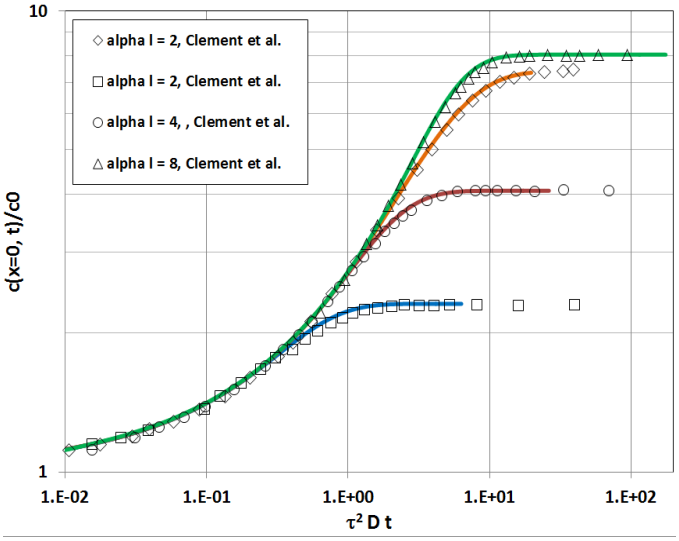


Fig. 2 Vacancy concentrations build up at the blocking boundary x = 0 for the finite length interconnect vs time at temperature T = 220°C and without temperature gradient effects. Solid lines are results from implemented model and symbols are results from Clement et al. [14]. (alpha l) in the legend represents αl, where l is the length of the interconnect. (◊) represents results using BCs Eq. 16 and 17, whereas (□,○,Δ) represents results using BC Eq. 16 for both end of the interconnect.

These MTF models and by including temperature gradient terms in Eqs. 4-14, the MTF model with temperature gradient effects will be similar to Eq. 1. In this paper we will not attempt to derive such form for temperature gradient effects but merely to show the effects of temperature gradient effects via FEA simulation. In fact, values of 6 to 7 for current density exponents for various EM experiments have been reported in the literature [5].

Governing Equations 8-19 are implemented in COMSOL Mutliphysics® software using the mathematics PDE module interface. Figure 2 shows simulation results for vacancy concentrations build up for finite length EM interconnect such as in Fig. 1 with the blocking boundary x = 0 for the finite length interconnect vs time at temperature T = 220°C. Temperature gradient and stress gradient terms are ignored to compare with the results of Clement et al. [15] to verify the implemented model.

Second example considered here for model verification is the Blech structure geometry with Aluminum interconnects and Tungsten-filled vias [16] is shown in Fig. 3a. Voltage of 0.3V is applied at the cathode such that average current density is 6 x $10^5$ A/cm$^2$. Figure 3b shows the current density crowding in the corner of the Aluminum/Tungsten interfaces. The maximum temperature is 184°C in the Tungsten vias and 176°C in the upper Aluminum interconnect is shown in Fig. 3c. Maximum hydrostatic stress is 88.5 MPa at the Aluminum/Tungsten interfaces shown in Fig. 3d. Figure 3e shows the normalized vacancy concentration with respect to initial concentration at the end of 277.78 hours. This shows that voids are accumulated at the cathode side of the Aluminum interconnects which verifies the implemented model with the well-known established fact that voids occurs at cathode end of the interconnects. Also note that EM is negligible in Tungsten-vias.

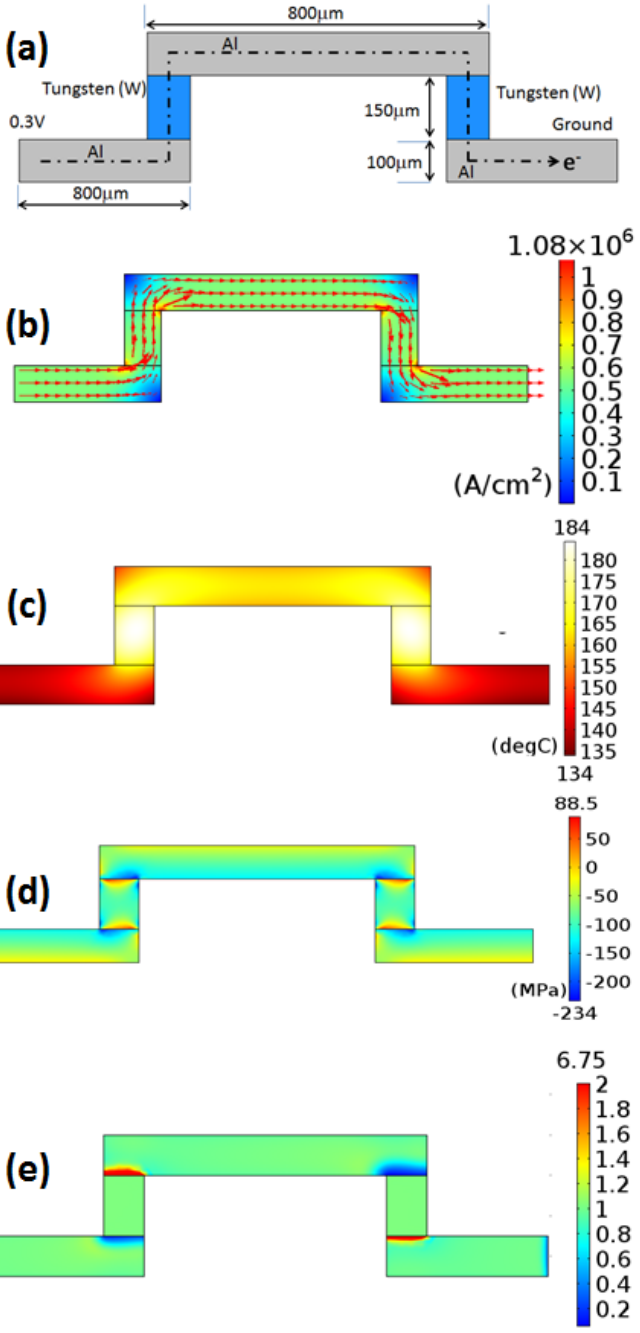


Fig. 3 Electromigration simulation of Blech structure with Aluminum interconnect and Tungsten-vias. (a) geometry description, (b) current density (c) temperature distribution, (d) hydrostatic stress distribution and (e) vacancy concentration at the end of 277.78 hrs.

## TEMPERATURE GRADIENT EFFECTS

Electromigration in flip-chip solder bumps can be critical for reliability due to shrinking in solder size, temperature rise and temperature gradient as these are far away from the heat sink. In this paper, flip-chip attached to a substrate geometry described in [17] is used to study influence of the temperature gradient on the EM for C4 solder bumps. The global model geometry shown in Fig. 4a and finite element mesh for the same in Fig. 4b. The global model of the thermal management model provides global thermal and stress BCs to the local model shown in the Fig. 5. The under bump metallization (UBM) on the silicon side is Nickel (Ni). The diameter of the solder bump is 100µm and the height is 90µm. The material properties for the electro-thermo-mechanical analysis are shown in Table 2 [17]. The material properties for various materials in the solder bump structure pertaining to EM equations 8-15 are shown in Table 3. It should be noted that there is high degree uncertainty with regard to these values in the literature. Values are chosen from [11, 16, 18, 19].

The EM Analysis will be carried out for two cases by imposing temperature gradients across the solder bumps. First case consists of a temperature gradient of 170ºC on the chip side to 60ºC on the substrate side with average solder bump temperature of 157.7ºC and maximum solder bump temperature of 164.2ºC as shown in Fig.6. Second case is with uniform temperature of 165ºC. For both cases the maximum current density is equal to 53,200 A/m$^2$. For vacancy concentration diffusion, blocking BC Eq. 16 is used between different material interfaces assuming no diffusion between the metals. The Figs. 7 and 8 show the vacancy concentration after 555.5 hours for case 1 and case 2 respectively. In each of these figures, the four scales showing vacancy concentration is for solder, Ni, Cu and Al respectively. Results clearly shows that EM is more in solder than other metals. After 555.5 hours, EM in solder is greater for case 1 than case 2. This clearly shows that for same current density failure times could be lower for lower solder average temperature with higher temperature gradient (case 1) than for higher solder temperature with low temperature gradient (case 2).

## CONCLUSIONS

In this paper, influence of temperature gradient in interconnects due to Joule heating in 3D packaging on electromigration failure is presented. Black's MTF model relates exponentially to the temperature of interconnects which is assumed to be constant hence does not take into account temperature gradient. Theoretical results in the literature that shows the relationship between the Black's MTF model and governing equations of EM are highlighted. A multi material FEA model for predicting the vacancy concentration is demonstrated through COMSOL Mutliphysics® software. The developed electromigration model incorporates the driving force due to temperature gradient in addition to the effects of current density, vacancy concentration gradients and stress gradients with the interconnects and due to coefficient of thermal expansion mismatch with surrounding materials. It is shown that for same current density in the complex C4 solder bumps of flip-chip packages it is possible that failure times could be lower for lower solder average temperature with higher temperature

gradient than for higher solder temperature with low temperature gradient.

Table 2. Material Properties for the Electro-thermo-Mechanical Models Eqs. 4-7.

| Materials | CTE (ppm/oC) | E (GPa) | υ | Yield (MPa) |
|---|---|---|---|---|
| Chip (Si) | 2.8 | 131 | 0.3 | |
| Passivation ($Si_3N_4$) | 2.9 | 325 | 0.24 | |
| Bond pad (Al) | 23.2 | 70 | 0.24 | |
| UBM layer 1 (Cu) | 16 | 117 | 0.3 | |
| UBM layer 2 (Ni) | 12.7 | 200 | 0.31 | |
| Solder bump (63Sn/37Pb) | 21 | 30 | 0.35 | 20 |
| Substrate (FR4) | 18 | 22 | 0.28 | |
| Underfill | 33 | 8.5 | 0.28 | |

Table 3. Electromigration Material Properties for Eqs. 8-12.

| Mat. | $Z^*$ | $Q^*$ (eV) | $f$ | $\Omega$ ($m^3$/atom) | $D_0$ ($cm^2$/s) | $Q$ (eV) |
|---|---|---|---|---|---|---|
| Al | -30 | 9.4e-3 | 1 | 2.48e-29 | 0.052 | 0.9 |
| Cu | -5 | 5.5 | 1 | 1.18e-29 | 0.6e-6 | 1.06 |
| Ni | -5 | 0.276 | 1 | 1.09e-29 | 0.0037 | 0.85 |
| Solder | -18 | 9.4e-3 | 1 | 2.72e-29 | 10.7 | 1.088 |
| W | -20 | 9.4e-3 | 1 | 2.48e-29 | 5.2e-4 | 1.0 |

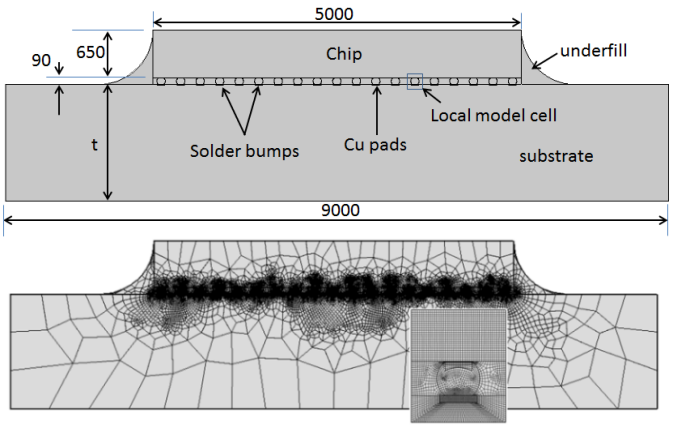


Fig. 4 (a) Geometry of the flip-chip package with solder bumps and copper pads for the global model, (b) finite element mesh for the global model with the zoom in section of solder bumps of the copper pad mesh.

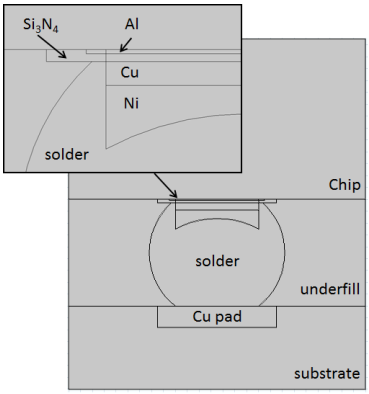


Fig. 5 Geometry of the flip-chip package with solder bumps, copper pads with UBM for the local model.

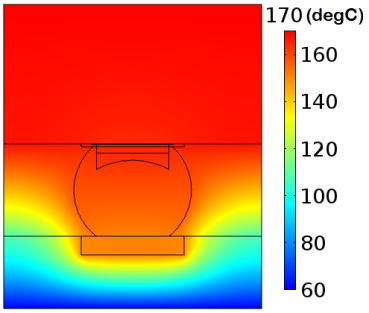


Fig. 6 Temperature distribution for case 1 with average temperature in the solder is 157.7°C.

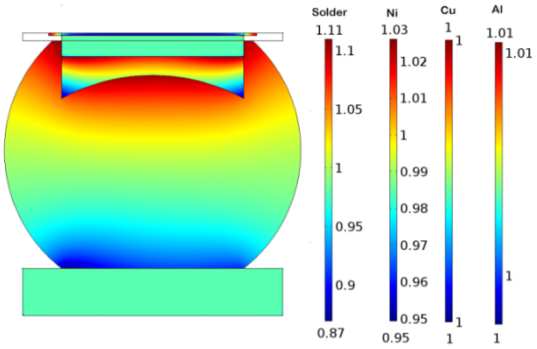


Fig. 7 Vacancy concentration in solder, Ni, Cu and Al for the case of average temperature in solder is 157.7°C.

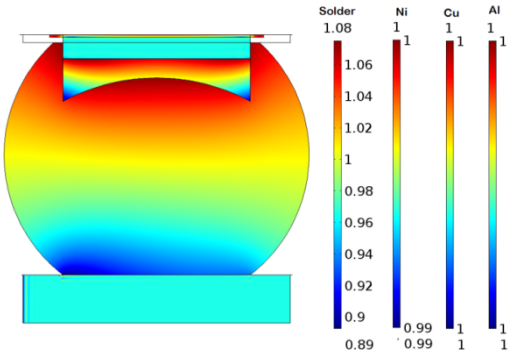


Fig. 8 Vacancy concentration in solder, Ni, Cu and Al for the case of average temperature in solder is 165°C.

**References**


[1] Black, J. R., Electromigration – A Brief Survey and Some Recent Results, IEEE Transactions on Electron Devices, Vol. 16, no. 4, pp. 338-347, 1969.

[2] International Technology Roadmap for Semiconductors (ITRS), 2013, Edition, 2011 Edition, Online: www.itrs.net/reports.html, 2011, 2013.

[3] Lienig, J., Electromigration and Its Impact on Physical Design in Future Technologies, 2013 ACM International Symposium on Physical Design (ISPD), pp. 33-40, 2013.

[4] Teng, C.-C., Cheng, Y.-K., Rosenbaum, E., and Kang, S.-M, iTEM: A Temperature-dependent Electromigration Reliability Diagnosis Tool, IEEE Trans, Comput.-Aided Des. Integr. Circuits Syst., Vol. 16, no. 8, pp. 882-893, Aug. 1997.

[5] Blair, J. C., Ghate, P. G., Haywood, C. T., Concerning Electromigration in Thin Films, Proc IEEE Lett, vol. 57, no. 9, pp. 1578 – 1594, 1971.

[6] Lloyd, J. Electromigration Failure, J. Appl. Phys., vol., 69, no. 11, pp. 7601-7604, 1991.

[7] Korhonen, M. A., Bogesen, P., Tu, K. N. and Li, C.-Y., Stress Evolution due to Electromigration in Confined Metal Lines, J. Appl. Phys. Vol. 73, no.8, pp. 3790-3799, 1993..

[8] Zhijian, L., Huang, W., Stan, M. R., Skadron, K., Lach., J. Interconnect Lifetime Prediction for Reliability-Aware Systems, IEEE Transactions on Very Large Integration Systems, vol. 15, no. 2, February 2007.

[9] Thematique J., From Power Packages to 3D Integration: The Thermal Challenge, STM Microelectronics,
Online: http://www.sft.asso.fr/

[10] Banerjee, K. and Mehrotra, A., Global [Interconnect] Warming, Circuits and Devices Magazine, IEEE, Vol. 17, no5, pp 16-32, 2001.

[11] Chao, B, Chae, S.C., Zhang, X., Lu K., Im J. and Ho P.S., Investigation of Diffusion and Electromigration Parameters for Cu-Sn Intermetallic Compounds in Pb-free Solders Using Simulated Annealing, Acta Materialia, Vol. 55, pp. 2805-2814, 2007.

[12] Tu, K. N., Recent Advances on Electromigration in Very-Large-Scale-Integration of Interconnects, Journal of Applied Physics, Vol. 94, no. 9, pp. 5452—5473, 2003.

[13] Shatzkes, M., Lloyd, J., A Model for Conductor Failure Considering Diffusion Concurrently with Electromigration Resulting in a Current Exponent of 2. J. Appl. Phys. Vol. 59, no. 11, pp. 3890—3893, 1986.

[14] Clement, J. J. and Lloyd, J. R., Numerical Investigations of the Electromigration Boundary Value Problem, J. Appl. Phys. Vol. 71, pp. 1729, 1992.

[15] Clement, J.J., Electromigration Modeling for Integrated Circuit Interconnect Reliability Analysis, IEEE Transactions on Device and Materials Reliability, Vol. 1, no. 1, pp. 33-42, March 2001.

[16] Zhu., X. Kotadia, H., Xu, S., Lu., H., Mannan., S. H., Bailey. C., Chan, Y.C., Progress in the Developments of an Electro-Migration Modeling Methodology, Processing of Blucher Mechanical Engineering, vol. 1, no. 1, May 2014.

[17] Gu, Y., Nakamura, T., Chen W., T., and Cotterell, B., Interfacial Delamination Near Solder Bumps and UBM in Flip-Chip Packages, Journal of Electronic packaging, vol., 123, pp. 295 – 301, Sep. 2001.

[18] Pharr., M., Zhao, K., Suo, Z., Ouyang, F.-Y., and Liu, P., Concurrent Electromigration and Creep in Lead-free Solder, Journal of Applied Physics, vol. 110, 083716, 2011.

[19] Butrymowicz, D., B., Manning, J., R., and Read., M., E., Diffusion in Copper and Copper Alloys. Part I. Volume and Surface Self-Diffusion in Copper, J. Phys. Chem. vol. 2, pp. 643, 1973, http://dx.doi.org/10.1063/1.3253129